Environ. Sci. Technol. **2009,** *43,* 3162–3168

White-Rot Basidiomycete-Mediated Decomposition of C_{60} Fullerol

KATHRYN M. SCHREINER,[†] TIMOTHY R. FILLEY,*[,†] ROBERT A. BLANCHETTE,[‡] BRENDA BEITLER BOWEN,[†] ROBERT D. BOLSKAR,[§] WILLIAM C. HOCKADAY,[||] CAROLINE A. MASIELLO,[||] AND JAMES W. RAEBIGER[§]

Department of Earth and Atmospheric Sciences, Purdue University, West Lafayette, Indiana 47907, Department of Plant Pathology, University of Minnesota, St Paul, Minnesota 55108, TDA Research, Wheat Ridge, Colorado, 80033, and Department of Earth Science, Rice University, Houston, Texas 77005

Received July 7, 2008. Revised manuscript received February 12, 2009. Accepted February 23, 2009.

Industrially produced carbon-based nanomaterials (CNM), including fullerenes and nanotubes, will be introduced into the environment in increasing amounts in the next decades. One likely environmental chemical transformation of C_{60} is oxidation to C_{60} fullerol through both abiotic- and biotic-mediated means. Unfortunately, knowledge of the environmental fate of oxidized CNM is lacking. This study used bulk and compound-specific ^{13}C stable isotope ratio mass spectrometry techniques and spectroradiometry analysis to examine the ability of two white rot basidiomycete fungi (*Phlebia tremellosa* and *Trametes versicolor*) to metabolize and degrade an oxygenated CNM, C_{60} fullerol. After 32 weeks of decay, both fungi were able to bleach and oxidize fullerol to CO_2. Additionally, the fungi incorporated minor amounts of the fullerol carbon into lipid biomass. These findings are significant in that they represent the first report of direct biodegradation and utilization of any fullerene derivative and provide valuable information about the possible environmental fates of other CNM.

Introduction

It is anticipated that industrially produced carbon-based nanomaterials (CNM), including fullerene (C_{60}) and its functionalized derivatives, will become widely distributed in the environment in this next century as the number of commercial applications of these products is expanding (*1*, *2*). Toxicological research on C_{60} and functionalized C_{60} has demonstrated a wide range of possible impacts to microbial and mammalian physiologies. There are a limited number of studies assessing the toxicity of polyhydroxylated fullerene, or C_{60} fullerols (*3*−*5*). For example, zebrafish embryos exposed to an aqueous solution (50 mg/L fullerols) exhibited no toxic effects (*6*); however, human dermal fibroblasts and liver carcinoma cells exhibited increased toxic effects as the hydroxyl group density on the fullerol decreased (*4*). Fullerols have also been shown to induce membrane damage in mammalian liver tissue through the production of reactive oxygen species under UV light (*3*).

The physicochemical properties of fullerenes and their derivatives are the main determinants of their potential environmental fate. For example, the ability of C_{60} to cluster into nanoparticles (nC_{60}) in water greatly enhances their aqueous concentration above dispersed molecular C_{60} (*6*). Additionally, aqueous nC_{60} can be oxidized through exposure to ozone to chemical forms that include carbonyl, vinyl ether, and hydroxyl groups (*7*). The conversion of C_{60} to oxygenated forms such as fullerols results in a fundamental change to its potential environmental fate, as fullerols are highly water soluble (*8*−*10*) and form reactive oxygen species upon exposure to light (*11*). The potential for enzymatic biodegradation of CNM to produce oxygenated forms has recently been demonstrated in experiments using horseradish peroxidase and nanotubes (*12*). Additionally, there is potential for the direct release of oxygenated CNM, given their commercial application in areas such as drug delivery (*13*−*15*), an industry that is anticipated to expand. A schematic of the potential means of converting fullerenes to fullerols in the environment and likely environmental fates is shown in Figure 1. Because of their high water solubility and highly reactive surface chemistry, it is likely that the mean residence time of oxygenated CNM would be dramatically lower than that of underivatized analogs in soils, sediments, or aquatic systems.

It is important to note that C_{60} fullerol contains numerous isomers and that the type of C−O linkages can be in a variety of functional groups including sp^3−C−OH, sp^2−C−OH, hemiketals, and carbonyls, influencing potential toxicity and environmental reactivity. Table S1 in the Supporting Information contains a review of reported FTIR analysis of commercially available and synthesized fullerols highlighting this point.

Given the great diversity of microbes capable of decomposing highly condensed aromatic structures (*16*−*18*), the biodegradation of oxygenated CNM is likely to be one of the more important mechanisms for environmental transformation. Within soil and sediment systems the basidiomycete fungi are likely to be important degraders of these compounds as they are capable of degrading a wide variety of aromatic species, such as polycyclic aromatic hydrocarbons (e.g., (*19*)), lignin (*20*, *21*), coal (*22*, *23*), and biochar (*24*). Some white rot basidiomycete fungi, such as *Trametes versicolor*, can simultaneously degrade lignin and other aromatic compounds along with polysaccharides, while others, such as *Phlebia tremellosa*, selectively decay lignin (*20*). White rot decay of such aromatic substances is facilitated by a variety of extracellular nonspecific enzymes, such as manganese peroxidase, lignin peroxidase, and laccase (*25*, *26*) which not only oxidize but also promote polymerization. The latter possibility is an important point when considering the potential of chemical cross-linking of fullerols to soil and sediment organic matter (Figure 1). By their enzymatic action white rot basidiomycete fungi also bleach dark-colored aromatic compounds as has been illustrated in paper pulp processing (*27*, *28*). It has also been noted that the presence of lignin and lignin-like compounds induces the production of peroxidases and speeds up the bleaching and delignification process (*29*).

In this study, we examine the ability of two species of white rot basidiomycete fungi to degrade and metabolize synthetic C_{60} fullerols ($C_{60}(OH)_{19-27}$), either directly or as a

* Corresponding author phone: (765) 494-6581; e-mail: filley@purdue.edu.
[†] Purdue University.
[‡] University of Minnesota.
[§] TDA Research.
[||] Rice University.

10.1021/es801873q CCC: $40.75

Published on Web 03/26/2009

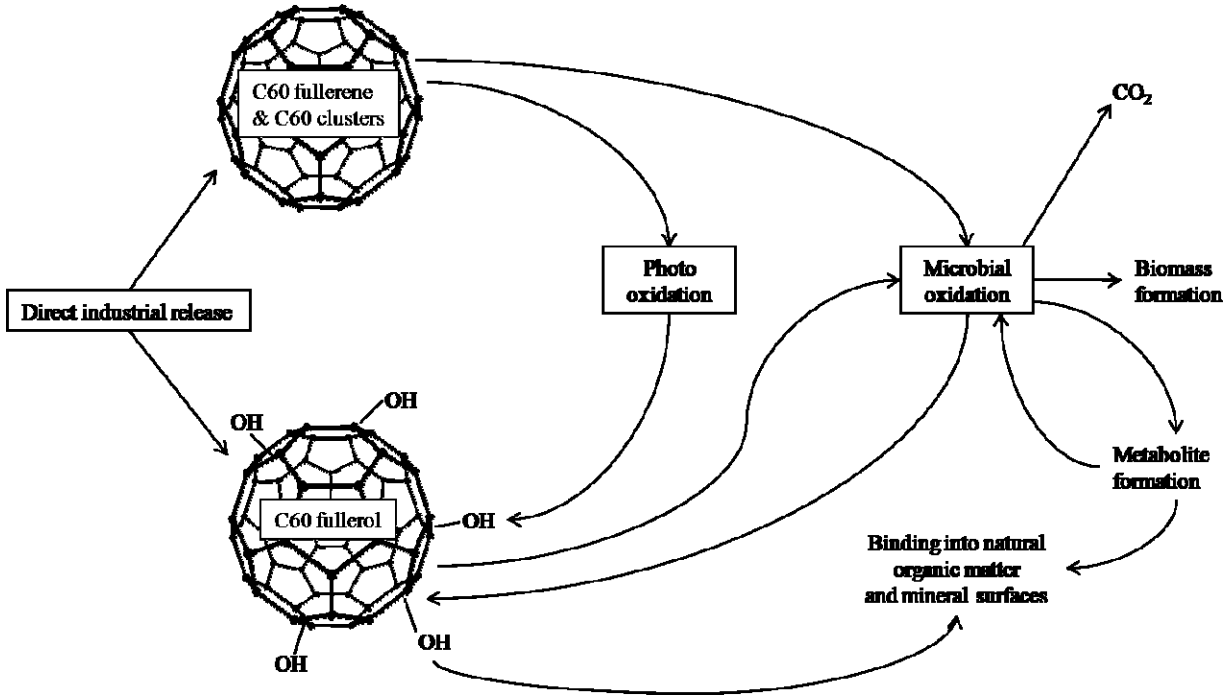

FIGURE 1. Overview of the potential environmental fates of fullerols.

result of cometabolic decay, in the presence of growth media and wood wafers, to further elucidate the fate of these important nanomaterials in natural environments.

Materials and Methods

Inoculation Experiments. The fungi *Trametes versicolor* (strain MAD 697-R) and *Phlebia tremellosa* (strain PRL 2845), maintained in the Forest Pathology and Wood Microbiology culture collection at the University of Minnesota, St. Paul, Minnesota, were chosen to test the ability of white rot basidiomycetes to degrade and metabolize fullerols. For each inoculation, approximately 15 mL of autoclaved 2% malt extract/agar media was added to a 50 mL clear glass jar (Scientific Specialties, Inc., Lodi, CA) with a hard plastic screw cap closure and a Teflon coated rubber septum. The influence of an autoclaved birch wood wafer was tested in half of the experiments, as wood can act as a trigger for the production of a wide array of ligninase enzymes as compared to growth in only culture media (*29, 30*). Wood (~350 mg dry weight) and fullerol (~35 mg at 22.32 atom % ^{13}C, synthesized at TDA Research as described in the Supporting Information) were added on top of a glass fiber filter disk (GF/F) which rested on top of the congealed media. The $C_{60}O_xH_y$, determined to contain 19−27 oxygen ($C_{60}(OH)_{19-27}$) atoms by solid state ^{13}CNMR as shown in Table S2, was placed either on the birch wafer (media + wood + fullerol experiments or MWF) or on top of the glass fiber filters (media + fullerol experiments or MF). The resultant percentage of fullerol C to total C in each jar was about 2.4% for MWF experiments and about 5.7% for the MF experiments. Fungal plugs were then added to all jars except controls such that they touched the fullerol and/or wood wafers as well as media. Experiments without fullerol and just media (M) and media with wood (MW) were also conducted. Three replicates of each experiment type (M, MW, MF, and MWF) for both fungal species (*T. versicolor* and *P. tremellosa*), as well as three replicates of MW and MWF for no fungal controls, were inoculated. One of the *T. versicolor* MF replicates, however, failed to grow and was not considered in the final analysis. The fungi were allowed to colonize the fullerol for 32 weeks. Experiments were kept in the dark to limit light exposure and reactor lids were kept closed and opened only in a clean air bench to provide aeration every three weeks and allow inspection to ensure no visible bacterial colonies were present. Oxygen concentrations were not monitored but opening the reactors at this interval appeared to be sufficient to maintain growth rates, as determined from previous experiments, and also minimized possible bacterial contamination. At 16 weeks the headspace was sampled for CO_2 and a portion of the fungal hyphae were harvested for compound-specific stable carbon isotope analysis of fungal lipids (see below).

The dark colored $C_{60}(OH)_{19-27}$ is very hygroscopic and immediately upon its addition to the inoculation jars it began to dissolve. Within two weeks of inoculation, fullerol appeared to be uniformly distributed throughout the growth media in each experiment.

Reflectance Spectroscopy Measurements of Media and Fullerol. Spectral reflectance measurements (Analytical Spectral Device [ASD] Fieldspec 3 spectroradiometer) of inoculation media contents were taken after 32 weeks to assess the potential chemical alteration of the fullerols (details concerning spectral analysis can be found in the SI). Chemical change was manifested primarily in the 350−900 nm range. Two significant features were analyzed in that wavelength range in each sample (see Figure 2): (1) an absorbance minimum feature with differing wavelength values and depth for each sample, and (2) an inflection point leading out of the absorbance feature back up to highly reflective values for higher wavelengths. Continuum removal data manipulation (described in SI) was performed on the raw spectral data, which allowed these inflection points to be analyzed as maxima on the absorbance spectra (*31*).

Extraction and Structural Analysis of Fungal Lipids. Hyphae were sampled from the jars at 16 weeks and base extracted to remove and concentrate fatty acid lipids according to procedures modified from Wakeham and Pease (*32*). For gas chromatographic analysis fatty acids were converted to trimethylsiloxyl derivatives and their structures were analyzed using an HP 5890 gas chromatograph, containing a 5% phenyl polymethylsiloxane capillary column (30 m, 0.25 mm i.d. HP-5) interfaced with an HP 5971 quadropole mass spectrometer. The GC oven was programmed from 40 to 260 °C at 7 °C per minute and maintained for 6 min. Commercially available standards were used for

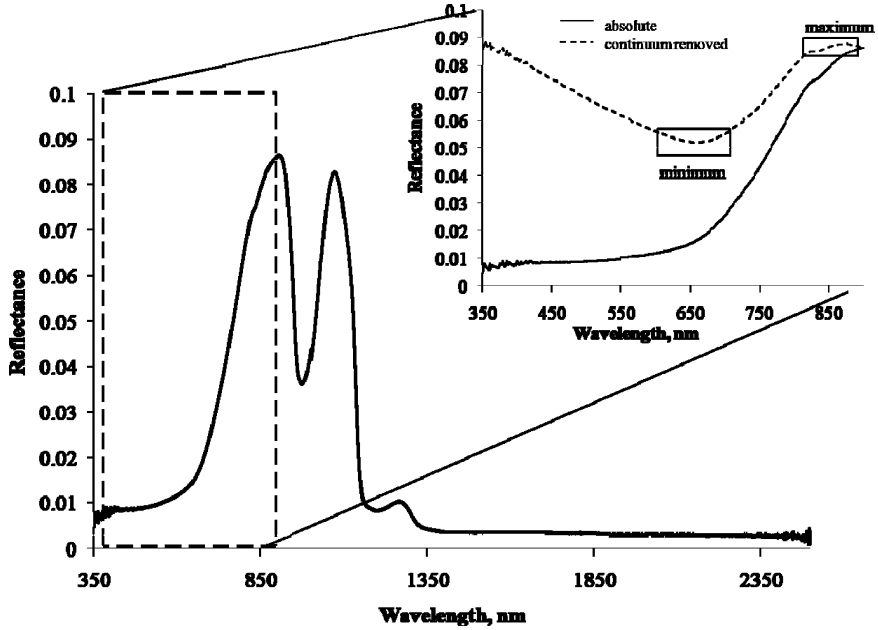

FIGURE 2. Example spectrum of absolute reflectance and continuum removed media + fullerol control sample. The inset shows the range used for analysis of the reflectance data, 350−900 nm. The minimum value represents the absorption feature seen for all samples, while the maximum value represents the inflection point as the spectrum moves to higher reflectance values.

reference. Both fungal species contain abundant 9,12-octadecadienoic acid, $C_{18:2}$ (*33*), and this was chosen as a marker to assess ^{13}C uptake into fungal biomass using analysis with compound specific gas chromatography−combustion−isotope ratio mass spectrometry (GC-C-IRMS).

Stable Carbon Isotope Ratio Monitoring Mass Spectrometry (IRMS). The fate of fullerol carbon was tracked using stable carbon isotope ratio monitoring of headspace CO_2, residual media and wood after 32 weeks decay, and the isolated fatty acid $C_{18:2}$ from the hyphae at the Purdue Stable Isotope (PSI) Facility. The fate of the ^{13}C-fullerol is discussed in terms of the % of C in the CO_2 and $C_{18:2}$ derived from the ^{13}C label in the MF and MWF experiments (eq 2, shown for $C_{18:2}$ MF-M comparison). Additionally, the percent of initial ^{13}C-fullerol C (IFC) remaining in the media or wood of each experiment after 32 weeks of decay was calculated by dividing the mass of fullerol C remaining in the media after 32 weeks by the mass of the initial fullerol C added (eq 3, shown for media). Details on the derivation of these equations can be found in the SI.

$$\%\ \text{C in } C_{18:2} \text{ from fullerol} = \frac{\text{atom } \%\ ^{13}C_{\text{MF lipid}} - \text{atom } \%\ ^{13}C_{\text{M lipid}}}{\text{atom } \%\ ^{13}C_{\text{pure fullerol}} - \text{atom } \%\ ^{13}C_{\text{M lipid}}} \times 100\% \quad (1)$$

$$\text{IFC}_{\text{media}} = \frac{\text{fullerol C at 32 weeks}_{\text{media}}}{\text{fullerol C at initial}_{\text{media}}} \times 100\% \quad (2)$$

Analysis of ^{13}C content of individual fatty acids was performed by GC-C-IRMS (*34*) on an Agilent 6890 GC interfaced to a PDZ-Europa 20/20 (SerCon Ltd., Crewe, U.K.) IRMS via a microcombustion furnace. The GC operating conditions were the same as described for structural analysis. Coinjection of eicosane as well as CO_2 pulses of known isotopic composition during the GC run were used to determine isotope drift and ^{13}C composition. The ^{13}C content of CO_2 produced by the fungi was measured at the end of 16 weeks at the time of sampling the hyphae. Headspace gases were removed in 500 μL aliquots from the inoculation jars with a gastight syringe and injected into helium-flushed 12 mL exetainer vials. The stable carbon isotope composition was determined using a SerCon (Crewe, U.K.) Cryoprep TG2 interfaced to a PDZ Europa 20/20 IRMS. Vials of CO_2 of known isotope composition were used as calibrants. Comparison of the ^{13}C content of CO_2 allowed for calculation of the fraction of CO_2 carbon that came from fullerol C as shown in eq 2. Wood and media from the jars were harvested after 32 weeks decay, dried at 60 °C, and ground for isotope analysis using a SerCon EA-CN 1 elemental analyzer interfaced to a PDZ-Europa 20/20 IRMS.

Statistical Treatment of Data. Differences in the extent of fullerol oxidation and incorporation of fullerol carbon into lipids were evaluated using two-tailed Student's *t* tests.

Results and Discussion

Evidence for Chemical Alteration of Fullerol by Reflectance Measurements. The two fungi used in the experiment have the capability to produce oxidative enzymes such as lignin peroxidase, manganese peroxidase, and laccase (*26, 35, 36*), which are known to oxidize aromatic plant-derived substances such as lignin (*20, 25*) as well as polycyclic aromatic substances (*19, 37, 38*). We anticipated that similar activity would be expressed in these experiments, and that fullerols would be oxidized and hydroxylated, causing a bleaching of the dark brown fullerol compound (*39*). By 32 weeks this bleaching was apparent both visually (see Figure S1) and by the total reflectance measurements (see Figure 3). In fact, even within 3 weeks of starting the fungal inoculations, it was noted that in the inoculated MWF experiments the media, darkened by fullerol, was lighter in color than the fullerol-containing media without fungi. Figure 3a and b illustrate the ability of these fungi to bleach the fullerol in media both in the presence of wood (panel a) and without wood (panel b). For *P. tremellosa* MW and *T. versicolor* M experiments (i.e., no fullerol added) samples, absorbance regions were shifted below 350 nm due to bleaching of the nutrients in the media, which is below the range of the spectroradiometer. These points are therefore not plotted in Figure 3.

In all experiments, both fungal species were able to bleach the fullerol, indicated by the shift to lower wavelength values for both the maximum and absorbance of the media after 32 weeks decay. Whereas the presence of the wood wafer was expected to increase the capacity of both fungi to bleach

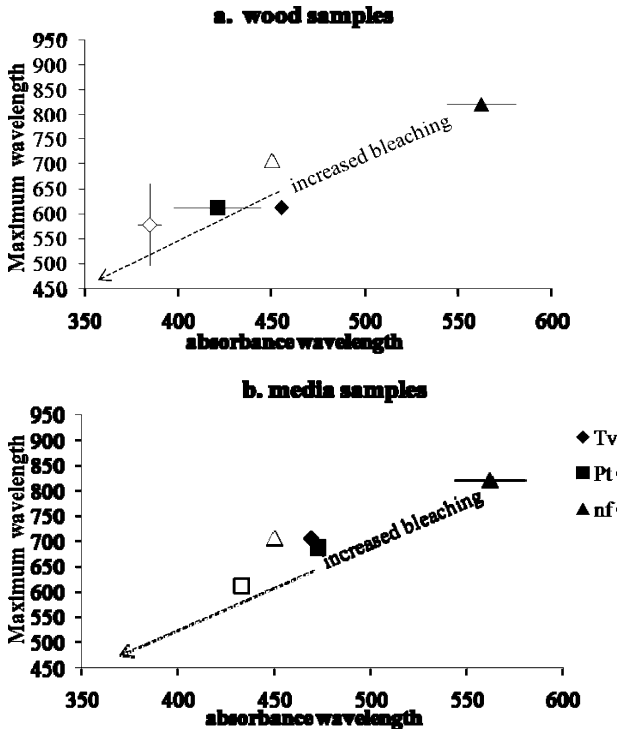

FIGURE 3. Absorbance feature comparison of wood (a) and media (b) inoculation experiment illustrating fungal alteration of spectral character of fullerol in media. Filled points represent samples with fullerol while open points represent samples with no fullerol. Tv: *T. versicolor*, Pt: *P. tremellosa*, nf: no fungus.

fullerol, only *P. tremellosa* exhibited enhanced bleaching in the presence of wood. This may be a function of the fungi responding differently to the nutrient levels provided by the growth media. By extrapolation, fullerols in the environment might be expected to exhibit greater alteration by some basidiomycete fungi when vascular plant carbon, most likely derived from lignin residues, is present. There are reported observations of enhanced oxidative decay in the presence of lignin (*29*), as well as polycyclic aromatic hydrocarbons and chlorinated phenols by white rot fungi (*40, 41*). During bleaching and delignification of wood pulps, a one electron oxidation of aromatic rings within the lignin is the first cause of decolorization (*29, 42*), and it is likely a similar phenomenon is occurring with the fullerol in the present experiments, with initial attack first on the hydroxyl functionality. In liquid culture agitated systems, the onset of lignin bleaching is reported to occur in 1−2 weeks (*36*), and solid-state cultures take longer for delignification to occur (*29*). A similar time frame for bleaching in our solid media samples was observed—after 2 weeks of fungal growth, the media had started to lighten.

Although the chemical structure of the altered fullerol cannot be directly assessed by spectroradiometry, the spectral shift seen in these experiments must be due to at least one of two phenomena: (1) removal of the sp^2-carbon on the fullerol by oxidation and cage rupture, resulting in lower molecular weight metabolites, or (2) increased hydroxylation of the sp^2-carbon, which has been shown to lighten the color of aqueous fullerol solutions (*39*). If the cage structure of the fullerol is oxidized into smaller fragments there exists the possibility that the fungi, or possibly other microbes in the natural environment, could utilize the fullerol carbon for biomass production or energy. The ^{13}C content of the CO_2 produced and the fungal lipids was used to test these possibilities (below).

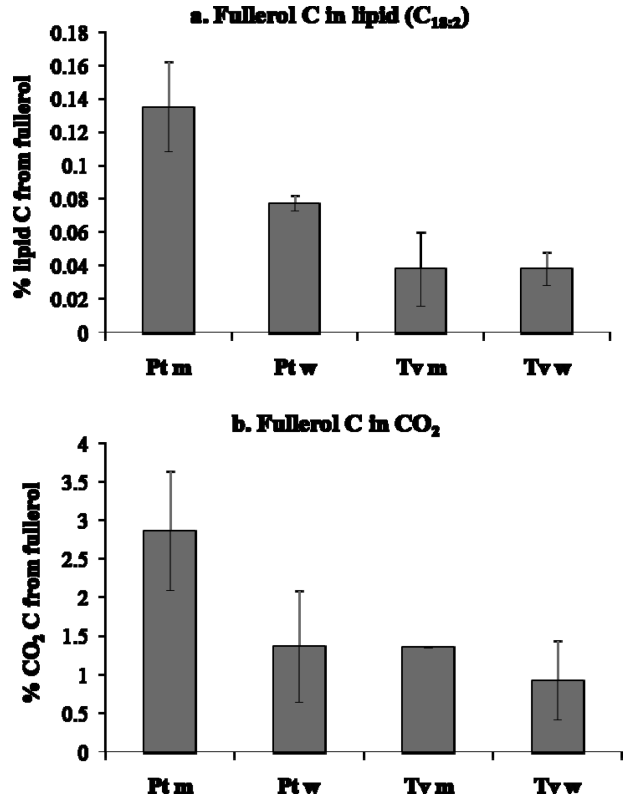

FIGURE 4. Bar graph depicts the percent of carbon in the $C_{18:2}$ fatty acid (a) and CO_2 (b) derived from added ^{13}C-labeled fullerol from both media and wood + media experiments. Tv: *T. versicolor*, Pt: *P. tremellosa*. Headspace CO_2 and fungal hyphae were sampled after 16 weeks inoculation.

Metabolic Fate of Fullerols (Biomass, CO_2, and Metabolites). Metabolized fullerol in this system has three possible fates: uptake into fungal biomass, oxidation to CO_2, or build-up of structurally and chemically altered products. Figure 4a shows the percentage of the C in the target lipid ($C_{18:2}$) derived from the ^{13}C fullerol. The data demonstrate these fungi are incorporating the fullerol carbon into fungal biomass, although only to a small degree. The fungus *P. tremellosa* incorporated a relatively greater percentage of ^{13}C fullerol carbon into $C_{18:2}$ than *T. versicolor* for both the MF ($p = 0.018$) and MWF ($p = 0.002$) experiments. For *P. tremellosa*, the $C_{18:2}$ from the MWF are comprised of less ^{13}C-fullerol C ($0.078 \pm 0.090\%$) than the MF experiments ($0.14 \pm 0.09\%$) ($p = 0.022$) while *T. versicolor* exhibited no difference between experiments with and without wood (~0.04%, $p = 0.987$). These differences may be a combination of different enzyme activities and the fact that the MWF experiments had more nonfullerol carbon available to the fungi. Considering these data and the relative loading of fullerol C in the decay experiments (ranging from 2.4 to 5.7% of total C) we can estimate that the fungi have a 20-fold (for the *P. tremellosa* MF experiment) to 142 fold (for the *T. versicolor* MWF experiment) preference for uptake of media or wood carbon over fullerol carbon. For the fullerol C to be taken up into this lipid the fullerol cage structure must be first broken down into acetate and reassembled to palmitic acid ($C_{16:0}$), which is the starting material for longer chain fatty acids (*43*). It is also possible that other anabolic products, e.g., sugars, proteins, etc., were formed in part from the fullerol C, although they were not analyzed. The minor capability of the fungi to convert the fullerol carbon to biomass in the presence of media is consistent with other findings on the activity of white rot fungi on lignin (*44*) and coal (*22, 24, 45*). Therefore, the bleaching of the fullerols (Figure 2 and Figure S1) observed in this study must be, in part, a function of

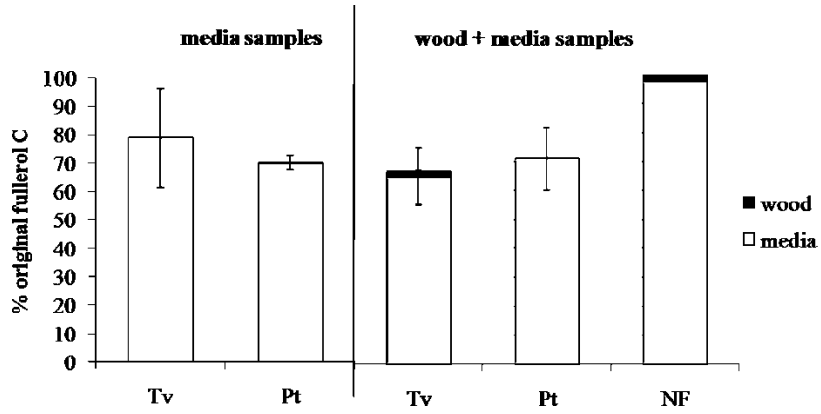

FIGURE 5. Distribution of the remaining ^{13}C-labeled fullerol C in the experiment at the close of the experiment. Error bars represent standard deviation of the three replicate samples for each type of experiment.

rupture of the cage and not simply increased hydroxylation (*39*). To the best of our knowledge, this is the first evidence for the biodegradability of these structures as well as the first evidence for their utilization in anabolic processes. This has important implications for the production of highly water soluble molecular fragments which may have an enhanced capability for further microbial consumption (*46*).

Sixteen weeks after the fungal inoculation began it was evident that some of the cage structure was being oxidized to CO_2 by the ^{13}C content of the CO_2 formed by the fungi (Figure 4b), which is consistent with the observed uptake of fullerol carbon into the fungal lipids. The calculated percentages of fullerol ^{13}C contributing to the CO_2 range from 1.35 ± 0.01% (*T. versicolor*) to 2.86 ± 0.78% (*P. tremellosa*) for MF experiments and 0.924 ± 0.516% (*T. versicolor*) to 1.36 ± 0.73% (*P. tremellosa*) for MWF experiments. *P. tremellosa* appears to be more aggressive toward oxidation of the fullerol cage carbon to CO_2 than T. versicolor (p = 0.081) for MWF experiments but not for the MF experiments. The greater capability of *P. tremellosa* to decompose as well as bleach the fullerol structure is consistent with other findings on the aggressive activity of this particular fungus on natural wood lignin (*20*) and also on synthetic lignin compounds (*47*). In contrast to the findings for the large discrimination against fullerol C uptake into lipids, the fungi show a lower preference for the media C over that of fullerol C when it comes to oxidation to CO_2. Specifically, *P. tremellosa* in the media experiment was only 2.0 times as likely to oxidize media C as it was fullerol C to CO_2, while *T. versicolor*, in its media fullerol decay experiment, exhibited the maximum discrimination against fullerol of 4.2 times. Carbon dioxide production from mineralization of substrate material by white rot fungi has also been observed during degradation of polycyclic aromatic hydrocarbons such as phenanthrene and pyrene (*48*), pentachlorophenol (*49*), and also of synthetic lignins (*47*).

The primary fate of the fullerol carbon after 32 weeks of decay, even though the spectral observations indicate substantial chemical bleaching, was as altered metabolites remaining in the media. Figure 5 shows distribution of the fullerol C remaining in these measured forms in the reaction jars at the end of the experiment. Among the replicates there was a wide range in the percentage of fullerol C remaining in the media but, in general, the two fungi showed similar responses among experiments with and without wood. Specifically, *T. versicolor* ranged from 61.1% to 96.1% initial fullerol C remaining dissolved in the media for the MF experiment and 54.4% to 74.1% for the MWF experiment while *P. tremellosa* ranged from 67.1% to 71.8% for MF and 63.5% to 78.7% for MWF. The remainder of the ^{13}C label, not accounted for in Figure 5, must be associated with the CO_2 loss and fungal hyphae produced, but unfortunately, neither was quantified for mass.

In general, the presence of wood in the experiments did not exhibit an influence on the amount of fullerol carbon remaining in the media as metabolites, although this was anticipated based upon known activity of fungi (*29*). The amount of the original ^{13}C-fullerol C remaining on the wood residue was always a minor component, <2.2% for all samples which was a function of both low wood recoveries because of enhanced decay, and dissolution of fullerols through the wood to the media. The no fungus fullerol control experiments indicate that although 100% of the fullerol was added to the top of the wood only 2.1% remained in the wood structure by 32 weeks. The remainder of the fullerol carbon accumulated in the media once it had diffused through the system.

Summary and Implications for Fullerols in the Environment. This study provides the first evidence of fullerol biodegradation and utilization. Both species of white rot fungi under these conditions could bleach fullerol as well as oxidize a small portion of it to CO_2, and incorporate it into fungal biomass. For *P. tremellosa*, the presence of wood appeared to enhance its ability to bleach the fullerol but not to decompose it to CO_2 nor incorporate it into biomass. The presence of wood for *T. versicolor* appeared to have little influence on decay dynamics. We can anticipate a range of activities among different species in nature and under different nutrient conditions but it is evident that if fullerols are produced in or released to the environment they have a great likelihood of being chemically altered by white rot fungi. Certainly further study is needed to determine the chemical structures of the bleached fullerol products as these will have a range of structure-dependent environmental fates. Additionally, fullerol degradation studies with natural soil communities and under nutrient limiting conditions would help determine the likely environmental fate of such compounds and inform future regulatory efforts.

Acknowledgments

We thank Benjamin Held and Joel Jurgens at the University of Minnesota for their help with the fungal laboratory experiments, David Gamblin and Sergey Oleynik at Purdue University for help on stable isotope measurements and lipids analysis, and Julie Petersen at TDA Research for assistance with the fullerol synthesis. We also acknowledge support from the National Science Foundation (NSF) under Award EEC-0404006, the United States Environmental Protection Agency (EPA) under STAR Grant, Award RD-83172001-0, and the National Institutes of Health (NIH) under Grant R01EB000703.

Supporting Information Available

Methodological details of the fullerol synthesis used in this study and its analysis by solid state ^{13}C NMR, spectroradiometry, and stable isotope measurements; table summarizing published FTIR spectral data on fullerols; table comparing the ^{13}C NMR of the fullerol synthesized for this study and a commercially available fullerol; figure illustrating the visual and spectroscopic evidence of fungal bleaching of fullerols from the inoculation experiments. This information is available free of charge via the Internet at http://pubs.acs.org.

Literature Cited

(1) Colvin, V. L. The potential environmental impact of engineered nanomaterials. *Nat. Biotechnol.* **2003**, *21* (10), 1166–1170.

(2) Murayama, H.; Tomonoh, S.; Alford, J. M.; Karpuk, M. E. Fullerene production in tons and more: From science to industry. *Fullerenes, Nanotubes, Carbon Nanostruct.* **2004**, *12* (1&2), 1–9.

(3) Kamat, J. P.; Devasagayam, T. P. A.; Priyadarsini, K. I.; Mohan, H. Reactive oxygen species mediated membrane damage induced by fullerene derivatives and its possible biological implications. *Toxicology* **2000**, *155*, 55–61.

(4) Sayes, C. M.; Fortner, J. D.; Guo, W.; Lyon, D.; Boyd, A. M.; Ausman, K. D.; Tao, Y. J.; Sitharaman, B.; Wilson, L. J.; Hughes, J. B. The differential cytotoxicity of water soluble fullerenes. *Nano Lett.* **2004**, *4* (10), 1881–1887.

(5) Zhu, X.; Zhu, L.; Li, Y.; Duan, Z.; Chen, W.; Alvarez, P. J. J. Developmental toxicity in zebrafish (*Danio rerio*) embryos after exposure to manufactured nanomaterials: Buckminsterfullerene aggregates (nC_{60}) and fullerol. *Environ. Toxicol. Chem.* **2007**, *26* (5), 976–979.

(6) Fortner, J. D.; Lyon, D. Y.; Sayes, C. M.; Boyd, A. M.; Falkner, J. C.; Hotze, E. M.; Alemany, L. B.; Tao, Y. J.; Guo, W.; Ausman, K. D. C_{60} in water: Nanocrystal formation and microbial response. *Environ. Sci. Technol.* **2005**, *39*, 4307–4316.

(7) Fortner, J. D.; Kim, D.-I.; Boyd, A. M.; Falkner, J. C.; Moran, S.; Colvin, V. L.; Hughes, J. B.; Kim, J.-H. Reaction of water-stable C_{60} aggregates with ozone. *Environ. Sci. Technol.* **2007**, *41*, 7497–7502.

(8) Chiang, L. Y.; Wang, L.-Y.; Swirczewski, J. W.; Soled, S.; Cameron, S. Efficient synthesis of polyhydroxylated fullerene derivatives via hydrolysis of polycyclosulfated precursors. *J. Org. Chem.* **1994**, *59*, 3960–3968.

(9) Li, J.; Takeuchi, A.; Ozawa, M.; Li, X. H.; Saigo, K.; Kitazawa, K. C_{60} fullerol formation catalysed by quaternary ammonium hydroxides. *J. Am. Chem. Soc., Chem. Commun.* **1993**, *23*, 1784–1785.

(10) Wang, S.; He, P.; Zhang, J.-M.; Jiang, H.; Zhu, S.-Z. Water-soluble [60]fullerenol by solvent-free reaction. *Synth. Commun.* **2005**, *35*, 1803–1808.

(11) Pickering, K. D.; Wiesner, M. R. Fullerol-sensitized production of reactive oxygen species in aqueous solution. *Environ. Sci. Technol.* **2005**, *127*, 799–805.

(12) Allen, B. L.; Kichambare, P. D.; Gou, P.; Vlasova, I. I.; Kaprolov, A. A.; Konduru, N.; Kagan, V. E.; Star, A. Biodegradation of single-walled carbon nanotubes through enzymatic catalysis. *Nano Lett.* **2008**, *8* (11), 3899–3903.

(13) Toth, E.; Bolskar, R. D.; Borel, A.; Gonzalez, G.; Helm, L.; Merbach, A. E.; Sitharaman, B.; Wilson, L. J. Water-soluble gadofullerenes: toward high-relaxivity, pH-responsive MRI contrast agents. *J. Am. Chem. Soc.* **2005**, *41* (3), 332–338.

(14) Anderson, S. A.; Lee, K. K.; Frank, J. A. Gadolinium-fullerenol as a paramagnetic contrast agent for cellular imaging. *Invest. Radiol.* **2006**, *41* (3), 332–338.

(15) Mikawa, M.; Kato, H.; Okumura, M.; Narazaki, M.; Kanazawa, Y.; Miwa, N.; Shinohara, H. Paramagnetic water-soluble metallofullerenes having the highest relaxivity for MRI contrast agents. *Bioconjugate Chem.* **2001**, *12*, 510–514.

(16) da Silva, M.; Cerniglia, C. E.; Pothuluri, J. V.; Canhos, V. P.; Esposito, E. Screening filamentous fungi isolated from estuarine sediments for the ability to oxidize polycyclic aromatic hydrocarbons. *World J. Microbiol. Biotechnol.* **2003**, *19* (4), 399–405.

(17) Dean-Ross, D.; Moody, J.; Cerniglia, C. E. Utilization of mixtures of polycyclic aromatic hydrocarbons by bacteria isolated from contaminated sediment. *FEMS Microbiol. Ecol.* **2002**, *41* (1), 1–7.

(18) Dean-Ross, D.; Cerniglia, C. E. Degradation of pyrene by *Mycobacterium flavescens*. *Appl. Microbiol. Biotechnol.* **1996**, *46* (3), 307–312.

(19) Marques-Rocha, F. J.; Hernandez-Rodriguez, V. Z.; Vazquez-Duhalt, R. Biodegradation of soil-adsorbed polycyclic aromatic hydrocarbons by the white rot fungus *Pleurotus ostreatus*. *Biotechnol. Lett.* **2000**, *22*, 469–472.

(20) Blanchette, R. A. Delignification by wood-decay fungi. *Ann. Rev. Phytopathol.* **1991**, *29*, 381–398.

(21) Leonowicz, A.; Matuszewska, A.; Luterek, J.; Ziegenhagen, K.; Wojtas-Wasilewska, M.; Cho, N.-S.; Hofrichter, M.; Rogalski, J. Biodegradation of lignin by white rot fungi. *Fungal Genet. Biol.* **1999**, *27*, 175–185.

(22) Cohen, M. S.; Gabriele, P. D. Degradation of coal by the fungi *Polyporus versicolor* and *Poria monticola*. *Appl. Environ. Microbiol.* **1982**, *44* (1), 23–27.

(23) Hofrichter, M.; Ziegenhagen, D.; Sorge, S.; Ullrich, R.; Bublitz, F.; Fritsche, W. Degradation of lignite (low-rank coal) by ligninolytic basidiomycetes and their manganese peroxidase system. *Appl. Microbiol. Biotechnol.* **1999**, *52*, 78–84.

(24) Hockaday, W. C.; Grannas, A. M.; Kim, S.; Hatcher, P. G. Direct molecular evidence for the degradation and mobility of black carbon in soils from ultrahigh-resolution mass spectral analysis of dissolved organic matter from a fire-impacted forest soil. *Org. Geochem.* **2006**, *37*, 501–510.

(25) Tuor, U.; Winterhalter, K.; Fiechter, A. Enzymes of white-rot fungi involved in lignin degradation and ecological determinants for wood decay. *J. Biotechnol.* **1995**, *41*, 1–17.

(26) Leonowicz, A.; Cho, N.-S.; Luterek, J.; Wilkolazka, A.; Wojtas-Wasilewska, M.; Matuszewska, A.; Hofrichter, M.; Wesenberg, D.; Rogalski, J. Fungal laccase: properties and activity on lignin. *J. Basic Microbiol.* **2001**, *41* (3−4), 185–227.

(27) Reid, I. D.; Paice, M. G. Effect of residual lignin type and amount on biological bleaching of kraft pulp by *Trametes versicolor*. *Appl. Environ. Microbiol.* **1994**, *60*, 1395–1400.

(28) Paice, M. G.; Jurasek, L.; Ho, C.; Bourbonnais, R.; Archibald, F. S. Direct biological bleaching of hardwood kraft pulp with the fungus *Coriolus versicolor*. *Tappi J.* **1989**, *72* (5), 217–221.

(29) Archibald, F. S.; Bourbonnais, R.; Jurasek, L.; Paice, M. G.; Reid, I. D. Kraft pulp bleaching and delignification by *Trametes versicolor*. *J. Biotechnol.* **1997**, *53*, 215–236.

(30) Shary, S.; Kapich, A. N.; Panisko, E. A.; Magnuson, J. K.; Cullen, D.; Hammel, K. E. Differential expression in *Phanerochaete chrysosporium* of membrane-bound proteins relevant to lignin degradation. *Appl. Environ. Microbiol.* **2008**, *74* (23), 7252–7257.

(31) Clark, R. N.; Roush, T. L. Reflectance spectroscopy: quantitative analysis techniques for remote sensing applications. *J. Geophys. Res.* **1984**, *89*, 6329–6340.

(32) Wakeham, S. G.; Pease, T. K. Lipid analysis in marine particle and sediment samples. Unpublished manuscript. 1992, pp 13−14.

(33) Stahl, P. D.; Klug, M. J. Characterization and differentiation of filamentous fungi based on fatty acid composition. *Appl. Environ. Microbiol.* **1996**, *62* (11), 4136–4146.

(34) Merritt, D. A.; Freeman, K. H.; Ricci, M. P.; Studley, S. A.; Hayes, J. M. Performance and optimization of a combustion interface for isotope ratio monitoring gas chromatography/mass spectrometry. *Anal. Chem.* **1995**, *67*, 2461–2473.

(35) Martinez, A. T.; Speranza, M.; Ruiz-Duenas, F. J.; Ferreira, P.; Camerero, S.; Guillen, F.; Martinez, M. J.; Gutierrez, A.; del Rio, J. C. Biodegradation of lignocellulosics: microbial, chemical, and enzymatic aspects of the fungal attack of lignin. *Int. Microbiol.* **2005**, *8* (3), 195–204.

(36) Reid, I. D.; Paice, M. G. Biological bleaching of kraft pulps by white-rot fungi and their enzymes. *FEMS Microbiol. Rev.* **1994**, *13*, 369–376.

(37) Bumpus, J. A. Biodegradation of polycyclic aromatic hydrocarbons by *Phanerochaete chrysosporium*. *Appl. Environ. Microbiol.* **1989**, *55*, 154–158.

(38) Vyas, B. R. M.; Bakowski, S.; Sasek, V.; Matucha, M. Degradation of anthracene by selected white rot fungi. *FEMS Microbiol. Ecol.* **1994**, *14*, 65–70.

(39) Kokubo, K.; Matsubayashi, K.; Tategaki, H.; Takada, H.; Oshima, T. Facile synthesis of highly water soluble fullerenes more than half covered by hydroxyl groups. *ACS Nano* **2008**, *2* (2), 327–333.

(40) Novotny, C.; Erbanova, P.; Sasek, V.; Kubatova, A.; Cajthaml, T.; Lang, E.; Krahl, J.; Zadrazil, F. Extracellular oxidative enzyme production and PAH removal in soil by exploratory mycelium of white rot fungi. *Biodegradation* **1999**, *10*, 159–168.

(41) Schmidt, K. R.; Chand, S.; Gostomski, P. A.; Boyd-Wilson, K. S. H.; Ford, C.; Walter, M. Fungal inoculums properties and its effect on growth and enzyme activity of *Trametes versicolor* in soil. *Biotechnol. Prog.* **2005**, *21*, 377–385.

(42) Michel, F. C.; Dass, S. B.; Grulke, E. A.; Reddy, C. A. Role of manganese peroxidases and lignin peroxidases of *Phanerochaete chrysosporium* in the decolorization of kraft bleach plant effluent. *Appl. Environ. Microbiol.* **1991**, *57* (8), 2368–2375.
(43) Abraham, W.-R.; Hesse, C.; Pelz, O. Ratios of carbon isotopes in microbial lipids as an indicator of substrate usage. *Appl. Environ. Microbiol.* **1998**, *64* (11), 4202–4209.
(44) Gleixner, G.; Danier, H.-J.; Werner, R. A.; Schmidt, H.-L. Correlations between the ^{13}C content of primary and secondary plant products in different cell compartments and that in decomposing basidiomycetes. *Plant Physiol.* **1993**, *102*, 1287–1290.
(45) Catcheside, D. E. A.; Mallett, K. J. Solubilization of Australian lignites by fungi and other microorganisms. *Energy Fuels* **1991**, *5*, 141–145.
(46) MacGillivray, A. R.; Shiaris, M. P. Relative role of eukaryotic and prokaryotic microorganisms in phenanthrene transformation in coastal sediments. *Appl. Environ. Microbiol.* **1994**, *60* (4), 1154–1159.
(47) Vares, T.; Niemenmaa, O.; Hatakka, A. Secretion of ligninolytic enzymes and mineralization of 14C-ring-labeled synthetic lignin by three *Phlebia tremellosa* strains. *Appl. Environ. Microbiol.* **1994**, *60* (2), 569–575.
(48) Sack, U.; Heinze, T. M.; Deck, J.; Cerniglia, C. E.; Martens, R.; Zadrazil, F.; Fritsche, W. Comparison of phenanthrene and pyrene degradation by different wood-decaying fungi. *Appl. Environ. Microbiol.* **1997**, *63* (10), 3919–3925.
(49) Tuomela, M.; Lyytikainen, M.; Oivanen, P.; Hatakka, A. Mineralization and conversion of pentachlorophenol (PCP) in soil inoculated with the white-rot fungus *Trametes versicolor*. *Soil Biol. Biochem.* **1999**, *31*, 65–74.

ES801873Q